Ice Sheet Elevation Change in West Antarctica from Ka-band Satellite Radar Altimetry

Inès Otosaka[1], Andrew Shepherd[1], and Malcolm McMillan[2]

[1]Centre for Polar Observation and Modelling, School of Earth and Environment, University of Leeds, LS2 9JT, UK.

[2]Centre for Polar Observation and Modelling, Lancaster University, LA1 4YW, UK.

Corresponding author: Inès Otosaka (eeino@leeds.ac.uk)

Key Points:

- AltiKa elevation is 3.8 ± 0.5 and 2.5 ± 0.1 m higher than airborne laser altimetry and CryoSat-2
- AltiKa elevation changes are 0.6 ± 2.4 and 0.1 ± 0.1 cm/yr lower than airborne laser and CryoSat-2, so trends in penetration are minor
- Surface lowering at the Pine Island Glacier has fallen by 9% since the 2000’s, while at Thwaites Glacier it has risen by 43%

Abstract

Satellite altimetry has been used to track changes in ice sheet elevation using a series of Ku-band radars in orbit since the late 1970's. Here, we produce an assessment of higher-frequency Ka-band satellite radar altimetry for the same purpose, using SARAL/AltiKa measurements recorded over West Antarctica. AltiKa elevations are 3.8 ± 0.5 and 2.5 ± 0.1 m higher than those determined from airborne laser altimetry and CryoSat-2, respectively, likely due to the instruments' coarser footprint in the sloping coastal margins. However, AltiKa rates of elevation change computed between 2013 and 2019 are within 0.6 ± 2.4 and 0.1 ± 0.1 cm/yr of airborne laser and CryoSat-2, respectively, indicating that trends in radar penetration are negligible. The fast-flowing trunks of the Pine Island and Thwaites Glaciers thinned by 117 ± 10 and 100 ± 20 cm/yr, respectively, amounting to a 9% reduction and a 43% increase relative to the 2000's.

Plain Language Summary

Satellite altimeters transmitting 2.3 cm radio waves have been used to track changes in the shape of Earth's polar ice sheets since the late 1970s. In this study, we demonstrate the capability of a new altimeter mission - SARAL/AltiKa - to survey ice in western Antarctica using shorter, 0.8 cm radio waves. AltiKa measures changes in elevation across most of the ice sheet to within 0.6 cm/yr of airborne and satellite sensors. Since the late 2000's, thinning of Thwaites Glacier has risen from 70 to 100 cm/yr, but thinning of Pine Island Glacier has fallen from 128 to 117 cm/yr.

1 Introduction

Satellite radar and laser altimetry have been widely used to derive ice sheet surface elevation and elevation change in Antarctica [e.g. *Wingham et al*., 1998, *Pritchard et al*., 2009; *Bamber et al*., 2009; *Slater et al*., 2018; *Schröder et al*., 2019; *Shepherd et al*., 2019] and in Greenland [e.g. *McMillan et al*, 2016; *Sandberg Sørensen et al*., 2018] to quantify their contributions to global sea level rise. Radar altimeters transmit pulses of electromagnetic radiation towards the Earth's surface and record the two-way travel time of the signal as well as the magnitude and the shape of the backscattered echo (waveform). The waveform shape is related to the average terrain and scattering properties of the Earth surface area illuminated by the altimeter footprint which, in turn, is determined by the sensor design [*Brown*, 1977]. The leading-edge position of the waveform can be deduced with the aid of an echo retracking algorithm [*Davis*, 1997; *Legresy et al*., 2005], and is typically used as a range adjustment to improve the precision of the surface elevation measurement.

The AltiKa sensor has operated on the ISRO/CNES SARAL satellite since 2013, and is the first space-borne radar altimeter transmitting at Ka-band (37 GHz, 0.8 cm wavelength) frequencies. In this study, we look at the strengths and weaknesses of this new dataset for cryosphere studies. In theory, Ka-band radar has a reduced penetration depth within ice sheet surfaces when compared to the Ku-band sensors (13.5 GHz, 2.3 cm wavelength) due to the scattering losses dominating in Ka-band (with a scattering coefficient ~57 times higher than in Ku-band) over absorption losses, and this has been supported by comparisons between the degree of radar backscattering recorded by AltiKa and ENVISAT over Antarctica [*Rémy et al*., 2015; *Adodo et al*., 2018]. Reduced signal penetration may potentially lead to better measurements of the ice sheets surface height. Previous studies have looked at the possibility of deriving elevation and elevation change in Antarctica [*Suryawanshi* et al., 2019] and Greenland [*Yang* et al., 2018] from AltiKa but their analyses were limited to only three years of data and did not include a comparison to Ku-band measurements. Here, we compute elevation and changes in the elevation of West Antarctica using 5 years of data acquired by AltiKa between March 2013 and March 2019. The main objectives of this study are to (i) assess the capability of AltiKa to measure elevation and elevation change in West Antarctica by comparing these estimates to contemporaneous airborne laser altimetry observations recorded by Operation IceBridge (OIB) and (ii) compare the Ka-band measurements to CryoSat-2 satellite Ku-band measurements to investigate whether the different frequencies of the two instruments lead to significant differences in elevation or elevation change.

2 Data and Methods

We use 51 million range measurements recorded by AltiKa between March 2013 and March 2019 to compute elevation change across the Amundsen Sea Sector of West Antarctica, a region that has exhibited widespread thinning [*Shepherd et al*., 2002; *Flament and Rémy*, 2012] due to ice dynamical imbalance [*Mouginot et al*., 2014; *Rignot et al*., 2019]. The range measurements were derived from 63 cycles of the AltiKa Sensor Geophysical Data Record (SGDR-T), and include corrections for dry tropospheric delay, wet tropospheric delay, ionosphere delay, solid earth tide, ocean loading tide and pole tide. The AltiKa data were acquired along the same 35-day repeat orbit as ERS-1/2 and ENVISAT until July 2016, date at which the satellite was moved to a drifting orbit because of technical issues on the reaction wheels [*Verron et al*., 2018]. This change of orbit did not affect the data availability or quality. Although AltiKa is a pulse-limited radar altimeter of similar design to ENVISAT, its operating bandwidth of 500 MHz allows for a higher pulse-repetition frequency (4 kHz) which allows a closer along-track sampling, a narrower beam width (0.6°), and a smaller (8 km diameter) ground footprint [*Steunou et al*., 2015; *Verron et al*., 2015].

To assess the performance of AltiKa, we compare the retrieved elevation and elevation change to satellite Ku-band altimetry data from CryoSat-2. CryoSat-2 is operating since 2010 and has been widely used to map the elevation and elevation change of the Greenland and Antarctic ice sheets [*Helm et al*., 2014; *Nilsson et al*., 2016]. It offers improved spatial coverage and resolution relative to previous pulse-limited altimeter missions, thanks to its high (92°) orbital inclination, its long-repeat drifting orbit, and – in coastal regions – its Synthetic Aperture Radar Interferometric Radar Altimeter (SARIn) mode [*Wingham et al*., 2006]. Over the interior of the ice sheets, CryoSat-2 operates as a traditional pulse-limited altimeter, known as Low-Resolution Mode (LRM).

Elevation measurements over the ice sheets need to be adjusted for the effects of the ice sheet surface slope, which typically ranges from 0.1° to 1.5° in Antarctica, introducing a 1.4 to 20.9 km lateral shift in the point of closest approach [*Brenner et al*., 1983; *Rémy et al*., 1989; *Levinsen et al*., 2016] or, equivalently, a 1.2 to 274.2 m error in the estimated elevation if the measurement was assumed to be originating from nadir. CryoSat-2 elevation measurements from Product L2I are corrected for this slope-induced error unlike AltiKa SGDR-T elevation measurements. To correct for this we apply a geometrical translation [*Roemer et al.*, 2007] that relocates echoes to the point of closest approach, using the same digital elevation model [*Liu et al*., 1999] employed in the ESA CryoSat-2 Level-2 processing chain to ensure a like-for-like comparison with CryoSat-2. In total, 76.1 % of echoes fall within AltiKa's beam-limited footprint. However, the remainder are in areas of high slope that tend to be located near to the ice sheet margin, which is a region of geophysical interest. To include these, we iterate the slope correction by artificially increasing the ground footprint diameter in three 1 km intervals, and this procedure allows us to retain 20.5 % more echoes (96.6 % in total).

We applied waveform retracker corrections to the AltiKa and CryoSat-2 range measurements to improve their precision. The shape of pulse limited satellite radar altimeter waveforms is dependent on the instrument specifications, the surface topography, and on the degree of surface and volume scattering [*Ridley and Partington*, 1988]. One aim of retracking algorithms is to mitigate the effects of volume scattering, which occurs if the radar pulse penetrates below the physical surface - as is common over ice sheets [*Michel et al*., 2014; *Nilsson et al*., 2015]. Retracking algorithms achieve this by identifying the location of the surface echo within the waveform, which is itself the sum of scattering from all elements illuminated by the transmitted pulse. A selection of retracker corrections are present within the AltiKa SGDR (ICE-1, ICE-2, Sea Ice and Ocean retrackers) and the CryoSat L2I (OCOG, Ocean CFI, UCL Land Ice retrackers) products and, for consistency, we pick similar ones for both missions. We choose Threshold Centre of Gravity (TCOG) based retracking algorithms [*Wingham et al*., 1986]: the ICE-1 retracker for AltiKa and the OCOG retracker for CryoSat-2 LRM waveforms. Only one waveform retracker (the Wingham/Wallis model fit) is available for CryoSat-2 data acquired in SARIN mode, and so we use this correction for those data [*ESA*, 2012].

We apply the same methodology to derive elevation and elevation change from AltiKa and CryoSat-2 [*McMillan et al*., 2014]. The data are collated within 5 km by 5 km square grid cells, and a multi-parameter least-square model fit is applied to retrieve the mean elevation and the mean rate of elevation change within each cell. The model fit accounts for the fluctuations in the heights recorded by the satellite, due to the horizontal location, the heading of the satellite, and time. We apply an additional correction on elevation change based on the correlation of elevation and backscattered power to account for temporal variability of the snowpack properties which can induce a spurious elevation change associated with changes in surface and volume scattering [*Davis and Ferguson*, 2004; *Simonsen and Sandberg Sørensen*, 2017]. We estimate the uncertainty in elevation from the departure between the heights recorded by the satellite and in our model fit. Errors in gridded rates of elevation change are estimated as the 1-sigma uncertainty from the linear fit, and errors over larger regions are computed as the sum in quadrature of this and the standard deviation of the elevation change measurements at each epoch over the contributing grid cells. Finally, we exclude grid cells where the time span of measurements is less than 2.5 years, where the magnitude of the elevation change rate exceeds 10 m/yr, where the root-mean-square of the residuals exceeds 10 m, or where the proportion of ascending and descending orbits is not evenly balanced.

To evaluate the accuracy of the AltiKa data, we use contemporaneous and coincident measurements of ice sheet elevation and elevation change acquired during NASA's Operation IceBridge (OIB) surveys. We use surface elevation measurements recorded by the NASA's Airborne Topographic Mapper (ATM) [*Studinger*, 2014a] (ILATM icessn) and elevation change rates derived from repeated ATM elevation measurements [*Studinger*, 2014b] (IDHDT).

3 Results

3.1 Comparison between Ka-band satellite altimetry and airborne laser altimetry

We computed the average surface elevation (Figure 1a) and the average rate of surface elevation change (Figure 1d) across the Amundsen Sea Sector between 2013 to 2019 from the AltiKa measurements alone. The region is an area of known dynamical imbalance [*Rignot*, 2008; *Mouginot et al*., 2014; *Joughin et al*., 2014] where rapid ice thinning has occurred across the coastal margins in the vicinity of its fast-flowing outlet glaciers [*Shepherd et al*., 2002]. Altogether, AltiKa is able to map 60.7 % of 5 km square grid cells within the study area (up to 81.5°), and most data gaps are small so that 95.7 % of the basin has an adjacent measurement at this resolution (see Figure S1). However, in areas of high slope, AltiKa struggles to track the ice sheet surface because of the instrument's smaller beamwidth and of the smaller range window explored (~40 m compared to ~ 60 m in LRM and ~ 120 m in SARIn for CryoSat-2). Furthermore, due to AltiKa's 35-day repeat cycle, the track spacing is wider compared to CryoSat-2 and only half (48.1 %) of grid cells falling on fast-flowing ice ($v > 250$ m/yr) are surveyed. For comparison, the interferometric altimeter of CryoSat-2 is able to survey 92.7% of the same ice [*McMillan et al*., 2018].

First, we compare AltiKa elevation measurements to the OIB measurements to evaluate their accuracy (Figures 1b and 1c). To compare the elevation data, we interpolated the satellite data to the time and location of the airborne measurements using the coefficients of the multi-parameter model fits, and we then computed the median difference within the 1,654 AltiKa data grid cells that contained at least five airborne measurements. We compare both the uncorrected and relocated AltiKa elevation measurements to OIB to assess the quality of our iterative slope correction. The uncorrected AltiKa measurements are positively biased with a median difference relative to OIB of 6.2 ± 0.5 m and associated standard deviation of 19.2 m. With our iterative relocation, the median difference is reduced to 3.8 ± 0.5 m with a standard deviation of 20.8 m. The OIB measurements are concentrated around the ice sheet margins (see Figure 1b), with 55.9 % of the data collected over surfaces with a slope higher than AltiKa's half antenna aperture (0.3°) where the median and standard deviation of the difference to OIB are 5.5 ± 0.8 m and 23.4 compared to 2.3 ± 0.5 m and 12.2 m in low slope areas. This larger departure from the OIB dataset in areas of slope exceeding 0.3° illustrates the trade-off between the beam width footprint of a radar altimeter and the slope of the terrain surveyed. There are advantages to a smaller footprint (e.g. a shaper waveform), however when the surface slope exceeds half the antenna aperture, the point of closest approach is shifted outside the beam footprint where the power is significantly lower. This does not apply to laser altimeters such as IceSat-1/2, which have footprints of the order of tens of meters over which the surface slope variations can be neglected. This could explain the positive bias and relatively high dispersion as 50.6 % of the echoes used in the comparison to OIB are scattered from beyond the instrument's 0.3° beam-limited footprint – 23.9 % of the total number of echoes across the study area – introducing an increased standard deviation in the difference to OIB of 17.8 m compared to 16.6 m when considering only the points within the 0.3° beam limited footprint. We also examine this elevation bias in terms of surface slope and roughness (see Figure S2). The differences between AltiKa and OIB exceeding 10 m are recorded in areas of slope higher than 0.4° and of surface roughness higher than 7 m. The presence of crevasses from which the returned echo is more complex could also potentially bias the elevation measurements recorded (Partington et al., 1987; Lacroix et al., 2007).

We also compared rates of surface elevation change computed from AltiKa data to those determined from the OIB measurements over 327 grid cells common to both datasets and falling within the CryoSat-2 SARIn mask (Figures 1e and 1f). Without a backscatter correction applied, the median difference between AltiKa and OIB rates of elevation change is -5.5 ± 2.5 cm/yr with an associated standard deviation of 43.0 cm/yr. Across this subset of grid cells, the backscatter correction applied to AltiKa elevation change is 4.8 cm/yr on average with a standard deviation of 30.7 cm/yr and across the study area as a whole, the magnitude of this correction is 1.0 cm/yr with a standard deviation of 16.5 cm/yr. Applying this correction leads to a better agreement with the laser altimetry rates of elevation change with a median difference of -0.6 ± 2.4 cm/yr and standard deviation of 42.7 cm/yr. This analysis shows that there is far better agreement between the OIB and AltiKa measurements of elevation change in comparison to elevation.

3.2 Comparison between Ka-band and Ku-band satellite altimetry

As a second test, we compared the AltiKa estimates of ice sheet surface elevation to independent estimates derived from CryoSat-2, to investigate potential differences in the degree of signal penetration recorded by each sensor. At the 3,580 common grid cells that contained at least five airborne measurements, the median difference between CryoSat-2 and OIB measurements of elevation is -0.7 ± 0.2 m, consistent with previous studies [*Slater et al*., 2018]. By comparison, the median difference between AltiKa and CryoSat-2 (computed as AltiKa - CryoSat-2) elevation data at 27,192 coincident grid cells is 2.5 ± 0.1 m, which confirms that AltiKa elevations are on average positively biased. Because the AltiKa bias is present in comparisons to both OIB and CryoSat-2, and because there is little evidence of bias between OIB and CryoSat-2, we do not believe it is associated with differences in the degree of radar penetration. Rather, the largest differences are in areas of high slope and roughness, suggesting this bias is related to the different instrument characteristics and in particular to the different footprint sizes and acquisition modes.

Next, we compared AltiKa and CryoSat-2 estimates of ice sheet surface elevation change to examine whether the positive bias in AltiKa elevation measurements is also present in the rates of elevation change recorded by AltiKa. This comparison also extends the area over which the AltiKa data can be evaluated with respect to independent observations, as the OIB data are limited to a small (< 2%) portion of the mainly coastal Amundsen Sea Sector. Across the region as a whole, the rate of elevation change recorded by AltiKa and CryoSat-2 averages 5.3 ± 1.0 cm/yr and 8.2 ± 1.2 cm/yr lowering between 2013 and 2019, respectively. Within the coastal margins (the SARIn mask of CryoSat-2, see Figure 1d), the average rate of surface lowering recorded by AltiKa and CryoSat-2 is 14.4 ± 1.6 cm/yr and 18.1 ± 2.0 cm/yr whereas in the interior (the LRM mask of CryoSat-2), the surface elevation increased at an average rate of 0.6 ± 0.6 cm/yr and 1.3 ± 1.0 cm/yr, respectively. At 27,192 common locations, the median difference between AltiKa and CryoSat-2 measurements of surface elevation change is -0.1 ± 0.1 cm/yr with an associated standard deviation of 11.5 cm/yr. This difference is small, and comparable to or smaller than the differences between each instrument and the OIB data themselves (-0.6 ± 2.4 cm/yr between AltiKa and OIB and -8.1 ± 1.5 cm/yr between Cryosat-2 and OIB, at 327 common grid cells). We also compute the robust dispersion estimate (RDE) of the difference between AltiKa and CryoSat-2 as defined by Smith et al. (2017). The RDE is 3.5 cm/yr and shows that although local differences exceeding 20 cm/yr do occur (e.g. Figure 3), the small regional differences suggest that there is no significant bias in either AltiKa and CryoSat-2 estimate of elevation change in this particular sector of Antarctica where the changes are dominated by changes in ice dynamics. Other factors that may be responsible for local differences between AltiKa and CryoSat-2 include differences in the low-level satellite data processing chains and differences in the satellite radar acquisition modes, and without equal treatment of these factors it is not possible to further isolate the potential effects of radar signal penetration.

We also compared AltiKa and Cryosat-2 rates of elevation change to Operation IceBridge along continuous sorties flown by the aircraft, to examine changes over diverse terrain in more detail: one along Thwaites Glacier, one along the centreline of Pine Island Glacier and another following approximately the ice sheet grounding line inland of the Getz Ice Shelf (see Fig. 1e). Along the Thwaites sortie, AltiKa records fewer measurements than Cryosat-2 but both sensors have comparable performances with RMS differences of 0.58 m/yr and 0.54 m/yr, respectively (Figure 2a). AltiKa and CryoSat-2 perform similarly well along the Pine Island Glacier sortie, yielding

RMS differences of 0.22 m/yr and 0.21 m/yr relative to OIB, respectively (Figure 2b). Along the Getz Ice Shelf sortie, however, AltiKa performs poorly due to the presence of steep and rough terrain, and acquires 9 times fewer measurements (Figure 2c). Although there is rapid thinning at several outlet glaciers, AltiKa fails to detect this, and records a RMS difference of 2.85 m/yr relative to OIB. This highlights the limits of AltiKa, which struggles to track surfaces in areas of complex terrain with rapidly changing slopes because of its smaller beam footprint and tracking window size, which are not very suited for high slope areas such as the ice sheet margins. Thus, deriving total volume change from AltiKa might be challenging, as most of the ice losses are occurring in the areas least well sampled by AltiKa. By comparison, the SARIn mode of CryoSat-2 performs extremely well despite the challenging terrain, tracking local thinning at a series of outlet glaciers along the sortie, with an RMS difference of 0.43 m/yr relative to OIB.

We also examined temporal variations in the surface elevation of the fast-flowing sections of Thwaites (Figure 3a) and Pine Island Glaciers (Figure 3b) recorded by AltiKa and CryoSat-2 to assess to which extent AltiKa can be used to examine elevation change trends at the scale of individual glaciers. Previous studies have identified rapid and increasing rates of surface lowering across the fast-flowing trunks of the Thwaites and Pine Island Glaciers [*Shepherd et al*., 2001; *Wingham et al.*, 2009]. This signal reflects glacier thinning associated with widespread ice dynamical imbalance [*Konrad et al*., 2016]. Observations recorded by AltiKa show that the surface at Thwaites Glacier has lowered at a rate of 100 ± 20 cm/yr between 2013 and 2019 and thinning exceeded 50 cm/yr at distances up to 173 km from the grounding line. Over Pine Island Glacier, AltiKa recorded a rate of elevation change of 117 ± 9 cm/yr over the same period with thinning spreading inland up to 363 km from the glacier's terminus. Thinning rates recorded at these two glaciers peaked at 343 ± 33 cm/yr and 216 ± 9 cm/yr at Thwaites and Pine Island Glaciers, respectively. We compared these Ka-band observations with CryoSat-2 data. Over Thwaites Glacier, CryoSat-2 is recording a rate of elevation change of 136 ± 14 cm/yr showing that AltiKa is slightly underestimating the elevation trend at this particular glacier, likely because AltiKa surveys only 45 % of the glacier, compared to an almost complete coverage of Thwaites Glacier (97 %) by Cryosat-2. On the other hand, the elevation change trend recorded by Cryosat-2 at Pine Island Glacier is in close agreement with AltiKa with a rate of 128 ± 9 cm/yr.

5 Discussion and Conclusions

We provide observations of ice sheet surface elevation change from Ka-band satellite radar altimetry. Using SARAL/AltiKa measurements and a least-square model fit, we map ice thinning across the Amundsen Sea Sector of West Antarctica between March 2013 and March 2019, and we evaluate these estimates using two independent datasets – Operation IceBridge airborne laser altimetry and CryoSat-2 satellite Ku-band radar altimetry. In general, the AltiKa, IceBridge, and CryoSat-2 data are in excellent agreement, with difference in elevation and elevation change in the range -59 to 68 m and -110 to 114 cm/yr for 99.7% of the data, respectively. We surmise that the small positive bias in elevation between AltiKa and IceBridge is related to AltiKa's coarser ground footprint and the sloping terrain of the study region. The slope correction we applied to the AltiKa dataset reduced this bias by 63% but a small residual slope effect remains. Despite being less suited to survey the ice sheets surface than CryoSat-2 because of its orbit inclination and smaller beam width compared to the magnitude of the slope found in the margins of the ice sheet, AltiKa is still able to detect elevation change with good levels of agreement with both airborne laser altimetry and Cryosat-2. The very small difference in elevation trends between AltiKa and IceBridge, and CryoSat-2 and IceBridge, is an indicator that trends in radar altimeter penetration are negligible in this region. Although deriving total volume change from AltiKa might be challenging, as it does not sample parts of the ice sheet margins where the surface slope and roughness are high with a sufficient spatial coverage, it is still able to detect changes in the surface elevation of Thwaites and Pine Island Glaciers for instance. The new Ka-band altimetry record presented in this study reveals that the surface elevation at Thwaites and Pine Island Glaciers has reduced by 7.9 ± 1.1 m and 6.8 ± 0.5 m respectively between 2013 and 2019 with a change in elevation of 2.5 ± 0.8 m and 2.3 ± 0.3 m in the last two years (2017-2019) of our survey. These additional two years of data added by our study to the long altimetry record already available show that the surface elevation lowering on Pine Island and Thwaites Glacier has continued at a similar pace compared to the 2013-2017 period. However, compared to surface elevation change estimates recorded during the 2000's from a combination of ERS-2 and ENVISAT (Shepherd et al., 2019), the rate of elevation change over the fast-flowing section of Thwaites Glacier has increased by 43 % and decreased by 9 % over Pine Island Glacier compared to the AltiKa record from 2013 to 2019. Overall, our study highlights the capability of AltiKa, the first space borne Ka-band altimeter, for measuring surface elevation change in West Antarctica.

Acknowledgments and Data

All SARAL/AltiKa data are freely available from AVISO at ftp://avisoftp.cnes.fr/AVISO/ and CryoSat-2 data are freely available from the European Space Agency at ftp://science-pds.cryosat.esa.int/. Operation IceBridge data were sourced from the National Snow and Ice Data Center at https://n5eil01u.ecs.nsidc.org/ICEBRIDGE/ILATM2.001/ (ILATM icessn) and https://n5eil01u.ecs.nsidc.org/ICEBRIDGE/IDHDT4.001/ (IDHDT). We are grateful to two anonymous reviewers and the editor, for their helpful comments on the manuscript.

References

Bamber, J.L., J.L. Gomez-Dans and J.A. Griggs (2009), A new 1 km digital elevation model of the Antarctic derived from combined satellite radar and laser data - Part 1: Data and methods, *Cryosphere*, 3(1), 101-111.

Brenner, A.C., R.A. Bindschadler, R.H. Thomas and H.J. Zwally (1983), Slope-induced errors in radar altimetry over continental ice sheets, *Journal of Geophysical Research: Oceans,* 88(C3), 1617-1623.

Brown, G. The average impulse response of a rough surface and its applications. *IEEE Transactions on Antennas and Propagation*, 1977, 25(1), 67-74.

Brunt, K.M., R.L. Hawley, E.R. Lutz, M. Studinger, J.G. Sonntag, M.A. Hofton, L.C. Andrews and T.A. Neumann (2017), Assessment of NASA airborne laser altimetry data using ground-based GPS data near Summit Station, Greenland, *Cryosphere*, 11(2), 681-692.

Davis, C.H. (1997), A robust threshold retracking algorithm for measuring ice-sheet surface elevation change from satellite radar altimeters, *IEEE Transactions On Geoscience And Remote Sensing*, 35(4), 974-979.

Davis, C. H. and A. C. Ferguson (2004), Elevation change of the Antarctic ice sheet, 1995-2000, from ERS-2 satellite radar altimetry, *IEEE Transactions on Geoscience and Remote Sensing*, 42(11), 2437-2445.

ESA: CryoSat-2 Product Handbook, ESRIN-ESA and Mullard Space Science Laboratory, University College London (2012), available at: http://emits.sso.esa.int/emits-doc/ESRIN/7158/CryoSat-PHB-17apr2012.pdf.

Flament, T. and F. Remy (2012), Dynamic Thinning of Antarctic Glaciers from Along-Track Repeat Radar Altimetry, *Journal of glaciology*, 58(211), 830-840.

Helm, V., A. Humbert and H. Miller (2014), Elevation and Elevation Change of Greenland and Antarctica Derived from Cryosat-2. *Cryosphere,* 8(4), 1539-1559.

Joughin, I., B. E. Smith and B. Medley (2014), Marine Ice Sheet Collapse Potentially under Way for the Thwaites Glacier Basin, West Antarctica. *Science*, 344(6185), 735-738. doi: 10.1126/science.1249055.

Konrad, H., Gilbert, L., Cornford, S., Payne, A., Hogg, A., Muir, A., and A. Shepherd (2017), Uneven onset and pace of ice-dynamical imbalance in the Amundsen sea embayment, west Antarctica, *Geophys. Res. Lett.*, 44(20), 910–918. doi:10.1002/2016GL07073.

Krabill, W., E. Hanna, P. Huybrechts, W. Abdalati, J. Cappelen, B. Csatho, E. Frederick, S. Manizade, C. Martin, J. Sonntag, R. Swift, R. Thomas and J. Yungel (2004), Greenland Ice Sheet: Increased coastal thinning, *Geophysical Research Letters*, 31(24), p.L24402.

Lacroix, P., B. Legrésy, R. COLEMAN, M. Dechambre and F. Rémy (2007), Dual-frequency altimeter signal from Envisat on the Amery ice-shelf, *Remote Sensing of Environment*, **109**(3), 285-294.

Legresy, B., Papa, F., Remy, F., Vinay, G., Van den Bosch, M. and O.Z. Zanife (2005), ENVISAT radar altimeter measurements over continental surfaces and ice caps using the ICE-2 retracking algorithm, *Remote Sensing Of Environment*, 95(2), 150-163.

Levinsen, J. F., S. B. Simonsen, L. S. Sorensen and R. Forsberg (2016), The Impact of DEM Resolution on Relocating Radar Altimetry Data Over Ice Sheets, *IEEE Journal of Selected Topics in Applied Earth Observations and Remote Sensing*, 9(7), 3158-3163.

Liu, H., K. C. Jezek and B. Li (1999), Development of an Antarctic digital elevation model by integrating cartographic and remotely sensed data: A geographic information system based approach, *Journal of Geophysical Research: Solid Earth*, 104(B10), 23199-23213.

McMillan, M., A. Shepherd, A. Sundal, K. Briggs, A. Muir, A. Ridout, A. Hogg, and D. Wingham (2014), Increased ice losses from Antarctica detected by CryoSat, *Geophys. Res. Lett.*, 41(11), 3899–3905. doi:10.1002/2014GL060111.

McMillan, M., Leeson, A., Shepherd, A., Briggs, K., Armitage, T.W.K., Hogg, A., Kuipers Munneke, P., van den Broeke, M., Noël, B., van de Berg, W. J., Ligtenberg, S., Horwath, M., Groh, A., Muir, A., and L. Gilbert (2016), A High-Resolution Record of Greenland Mass Balance: High-Resolution Greenland Mass Balance, *Geophys. Res. Lett*., 43(13), 7002-10.

McMillan, M., Shepherd, A., Muir, A., Gaudelli, J., Hogg, A. and R. Cullen (2017), Assessment of Cryosat-2 Interferometric and Non-Interferometric Sar Altimetry over Ice Sheets, *Advances in Space Research*.

Michel, A., T. Flament and F. Remy (2014), Study of the Penetration Bias of ENVISAT Altimeter Observations over Antarctica in Comparison to ICESat Observations, *Remote Sensing*, 6(10), 9412-9434.

Mouginot, J., E. Rignot, and B. Scheuchl (2014), Sustained increase in ice discharge from the Amundsen Sea Embayment, West Antarctica, from 1973 to 2013, *Geophys. Res. Lett*., 41(5), 1576–1584. doi:10.1002/2013GL059069.

Nilsson, J., P. Vallelonga, S.B. Simonsen, L.S. Sørensen, R. Forsberg, D. Dahl-Jensen, M. Hirabayashi, K. Goto-Azuma, C.S. Hvidberg, H.A. Kjaer and K. Satow (2015), Greenland 2012 melt event effects on CryoSat-2 radar altimetry: Effect Of Greenland Melt On Cryosat-2, *Geophysical Research Letters*, 42(10), 3919-3926.

Nilsson, J., A. Gardner, L.S. Sorensen and R. Forsberg (2016), Improved retrieval of land ice topography from CryoSat-2 data and its impact for volume-change estimation of the Greenland Ice Sheet, *Cryosphere*, 10(6), 2953-2969.

Partington, K., W. Cudlip, N. McIntyre and S. King-Hele (1987), Mapping of Amery Ice Shelf, Antarctica, Surface Features by Satellite Altimetry, *Annals of Glaciology*, *9*, 183-188. doi:10.3189/S0260305500000586

Pritchard, H. D., Arthern, R. J., Vaughan, D. G. and L.A. Edwards (2009), Extensive dynamic thinning on the margins of the Greenland and Antarctic ice sheets, *Nature*, 461(7266), 971-975. doi:10.1038/nature0847.

Remy, F., Mazzega, P., Houry, S., Brossier, C. and J. Minster (1989), Mapping of the Topography of Continental Ice by Inversion of Satellite-altimeter Data, *Journal of Glaciology*, 35(119), 98-107.

Rémy, F., Flament, T., Michel, A. and D. Blumstein (2015), Envisat and SARAL/AltiKa Observations of the Antarctic Ice Sheet: A Comparison between the Ku-band and Ka-band, *Marine Geodesy*, 38(sup1), 510-521. doi:10.1080/01490419.2014.985347.

Ridley, J. K. and K.C. Partington (1988), A model of satellite radar altimeter return from ice sheets, *Remote Sensing*, 9(4), 601-624. doi: 10.1080/01431168808954881

Rignot, E. (2008), Changes in West Antarctic Ice Stream Dynamics Observed with Alos Palsar Data, *Geophys. Res. Lett.*, 35(12).

Rignot, E., J.Mouginot, and B. Scheuchl (2011), MEaSUREs InSAR-Based Antarctica Ice Velocity Map, NASA DAAC at the Natl. Snow and Ice Data Cent., Boulder, Colo., doi:10.5067/MEASURES/CRYOSPHERE/nsidc-0484.001.

Sandberg Sørensen, L., Simonsen, S.B., Forsberg, R., Khvorostovsky, K., Meister., R. and M. Engdahl (2018), 25 Years of Elevation Changes of the Greenland Ice Sheet from Ers, Envisat, and Cryosat-2 Radar Altimetry, *Earth and Planetary Science Letters*, 495, 234-41.

Schröder, L., M. Horwath, R. Dietrich, V. Helm, van den Broeke, M. R. and S. R. M. Ligtenberg (2019), Four decades of Antarctic surface elevation changes from multi-mission satellite altimetry, *The Cryosphere* 13(2), 427-449.

Shepherd, A., D. J. Wingham, A. D. M. Justin and F. J. C. Hugh (2001), Inland Thinning of Pine Island Glacier, West Antarctica, *Science*, 291(5505), 862-864.

Shepherd, A., Wingham, D.J. and J.A.D. Mansley (2002), Inland Thinning of the Amundsen Sea Sector, West Antarctica, *Geophys. Res. Lett.*, 29(10), 1364-2-4.

Shepherd, A., L. Gilbert, A. S. Muir, H. Konrad, M. Mcmillan, T. Slater, K. H. Briggs, A. V. Sundal, A. E. Hogg and M. Engdahl (2019), Trends in Antarctic Ice Sheet Elevation and Mass, *Geophys. Res. Lett.*

Simonsen, S. B. and L. Sandberg Sørensen (2017), Implications of changing scattering properties on Greenland ice sheet volume change from cryosat-2 altimetry, *Remote Sensing of Environment*, 190, 2017-216. doi:10.1016/j.rse.2016.12.012.

Slater, T., A. Shepherd, M. McMillan, A. Muir, L. Gilbert, A. E. Hogg, H. Konrad and T. Parrinello (2018), A new digital elevation model of Antarctica derived from CryoSat-2 altimetry, *The Cryosphere*, 12(4), 1551-1562. doi: 10.5194/tc-12-1551-2018

Smith, B., N. Gourmelen, A. Huth and I. Joughin (2017), Connected subglacial lake drainage beneath Thwaites Glacier, West Antarctica, *The Cryosphere*, 11(1), 451-467. doi: 10.5194/tc-11-451-2017

Studinger, M. 2014, updated 2018. *IceBridge ATM L2 Icessn Elevation, Slope, and Roughness, Version 2*. [2013 to 2016] Boulder, Colorado USA. NASA National Snow and Ice Data Center Distributed Active Archive Center. doi: https://doi.org/10.5067/CPRXXK3F39RV.

Studinger, M. 2014, updated 2018. *IceBridge ATM L4 Surface Elevation Rate of Change, Version 1*. [2013 to 2016]. Boulder, Colorado USA. NASA National Snow and Ice Data Center Distributed Active Archive Center. doi: https://doi.org/10.5067/BCW6CI3TXOCY.

Suryawanshi, M. R., S. Chander, S. R. Oza, and I. M. Bahuguna (2019), Variability in the ice sheet elevations over Antarctica derived from repetitive SARAL/AltiKa radar altimeter data (2013–2016), *Journal of Earth System Science*, 128(3), 64, doi:10.1007/s12040-019-1093-x.

Verron, J., Sengenes, P., Lambin, J., Noubel, J., Steunou, N., Guillot, A., Picot, N., Coutin-Faye, S., Sharma, R., Gairola, R.M. & Murthy, D.R. (2015), The SARAL/AltiKa altimetry satellite mission. *Marine Geodesy*, 38(sup1), 2-21. doi:10.1080/01490419.2014.1000471.

Wingham, D. J., Rapley, C. G., and H. Griffiths (1986), New techniques in satellite altimeter tracking systems, *Proceedings of the IGARSS Symposium*, vol. SP-254, 1339–1344, edited by: Guyenne, T. D. and Hunt, J. J., European Space Agency, Zurich, September 1986.

Wingham, D.J., Ridout, A.J., Scharroo, R., Arthern, R.J. and C.K. Shum (1998), Antarctic elevation change from 1992 to 1996, *Science*, 282(5388), 456-458. doi:10.1126/science.282.5388.45.

Wingham, D., Francis, C. R., Baker, S., Bouzinac, C., Cullen, R., de Chateau-Thierry, P., Laxon, S. W., Mallow, U., Mavrocordatos, C., Phalippou, L., Ratier, G., Rey, L., Rostan, F., Viau, P. and D. Wallis (2006), CryoSat: a mission to determine the fluctuations in Earth's land and marine ice fields, *Adv. Space Res.*, 37, 841–871. doi:10.1016/j.asr.2005.07.027.

Wingham, D. J., D. W. Wallis and A. Shepherd (2009), Spatial and temporal evolution of Pine Island Glacier thinning, 1995–2006, *Geophysical Research Letters*, 36(17), L17501-np.

Yang, Q., Y. Yang, Z. Wang, B. Zhang and H. Jiang (2018), Elevation Change Derived from SARAL/ALtiKa Altimetric Mission: Quality Assessment and Performance of the Ka-Band. *Remote Sens.*, 10, 539.

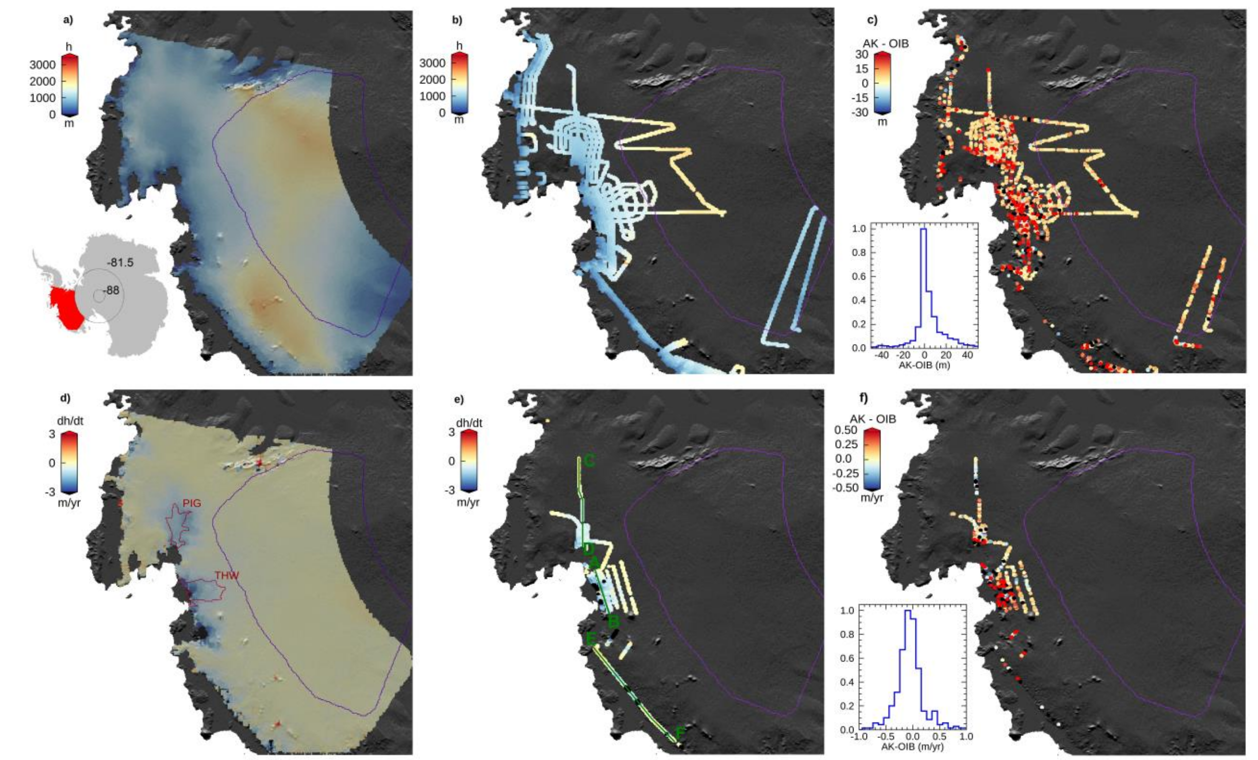

Figure 1. (a) Average elevation of the Amundsen Sea Sector determined from AltiKa Ka-band satellite radar altimetry between March 2013 and March 2019, h, (b) average elevation from Operation IceBridge airborne laser altimetry, (c) elevation difference between AltiKa and airborne laser altimetry, (d) average rate of elevation change from AltiKa, dh/dt, (e) average rate of elevation change from Operation IceBridge, (f) difference between rates of elevation change between AltiKa and airborne laser altimetry. The size of the OIB data has been increased for better visualization. A 25 km x 25 km median filter is applied to fill small gaps in the AltiKa data. The inset on (a) represents the location of the study area in Antarctica. Insets on (c) and (f) are histograms of the difference between AltiKa and OIB in the recorded elevation and rates of elevation change, respectively. Purple line shows the boundary between CryoSat-2 LRM and SARIn acquisition modes, green lines show OIB flight lines (A to B, C to D and E to F), and the red outlines mark the central trunks of the Pine Island (PIG) and Thwaites (THW) Glaciers defined by a 250 m/yr contour from ice velocity data [*Rignot et al*., 2011].

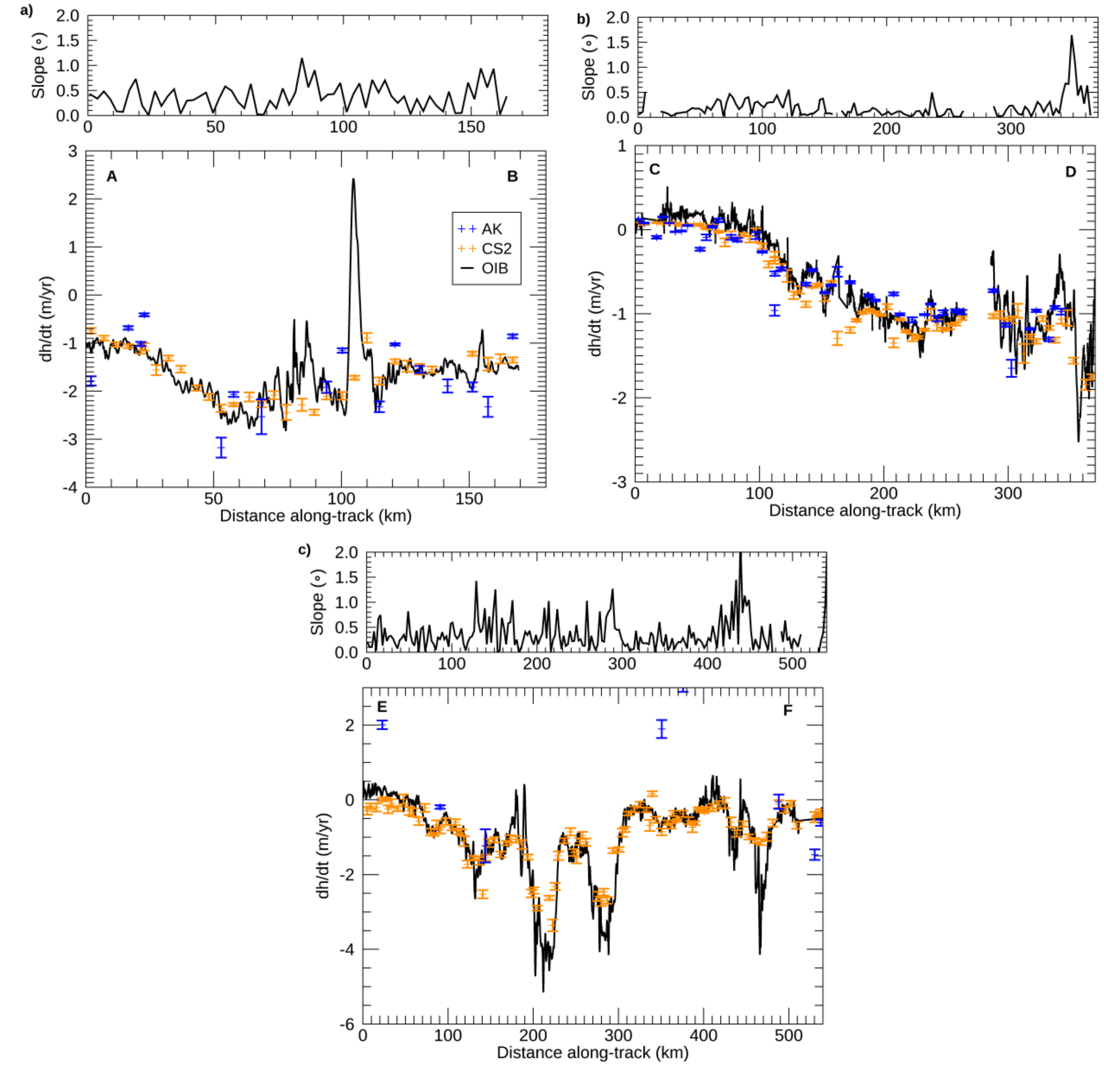

Figure 2. Rates of elevation change profiles from Operation IceBridge ATM, AltiKa and CryoSat-2 and ATM surface slope profiles (a) along airborne sorties of Thwaites Glacier from A to B, (b) Pine Island Glacier from C to D and (c) at the Getz Ice Shelf grounding line from E to F (locations shown on Figure 1e).

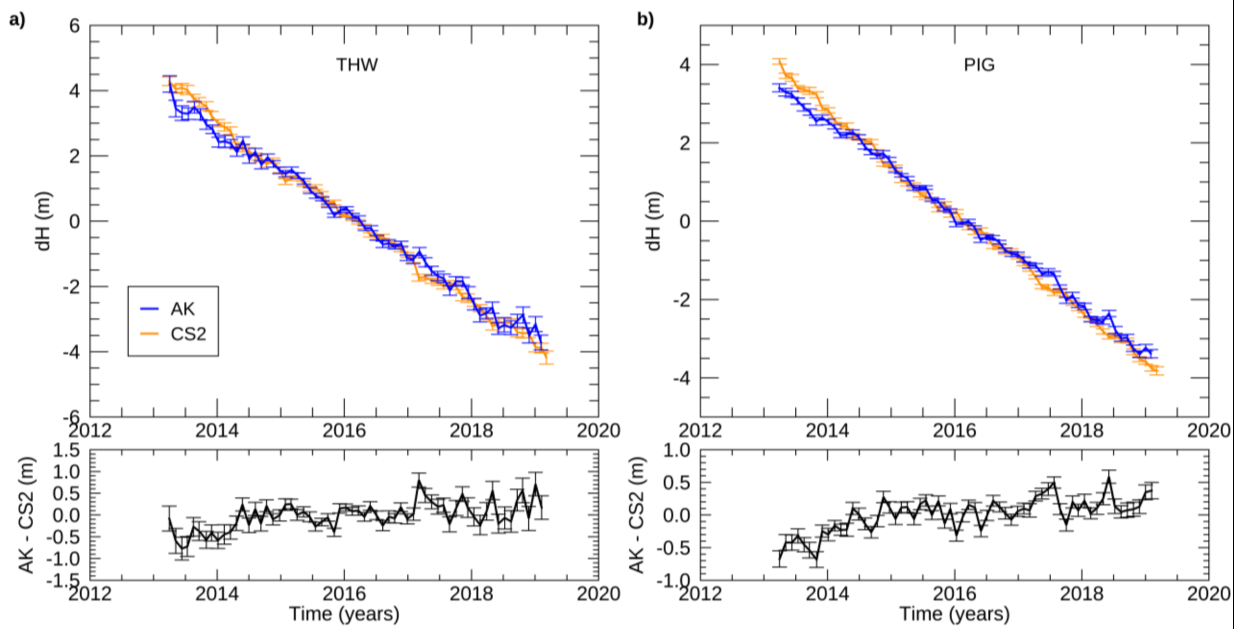

Figure 3. Time series of elevation change over (a) Thwaites Glacier and (b) Pine Island Glacier fast-flowing trunks (shown on Figure 1d) from AltiKa and CryoSat-2 and elevation change difference.